Waveform inversion for microseismic source parameters: Synthetic and field-data applications

Oscar Jarillo Michel and Ilya Tsvankin, Center for Wave Phenomena, Colorado School of Mines*

SUMMARY

Accurate estimation of the source parameters is a major task in microseimic monitoring. Here, we employ elastic waveform inversion (WI) to estimate the location, origin time, and seismic moment tensor of microseismic sources embedded in 2D VTI (transversely isotropic with a vertical symmetry axis) media. Forward modeling is carried out with a finite difference code that generates P- and SV-waves from dislocation-type sources. In addition to minimization of the objective function with a constant step length, we apply the nonlinear conjugate gradient method (NCG) for model updating. The WI algortihm is shown to be stable in the presence of moderate random Gaussian noise. We also present preliminary results of testing the WI methodology on a data set from Bakken field, North Dakota.

INTRODUCTION

Microseismic data are used to find the spatial and temporal distribution of hypocenters of events triggered during hydraulic stimulation and to estimate the source mechanisms (moment tensors). Conventional event-location techniques are based on picking the arrival times of the direct P- and S-waves in a borehole or at the surface (Rutledge and Scott, 2003). Also, microseismic events can be located without traveltime picking, by employing stacking (Anikiev et al., 2014), migration-based methods (Zhang and Zhang, 2013; Zhebel and Eisner, 2015), and waveform inversion (Kim et al., 2011; Jarillo Michel and Tsvankin, 2014a,b).

Event locations are usually determined by assuming the velocity model to be known, for example from perforation shots and borehole data. However, this approach may produce inaccurate results if there are errors in the velocity parameters, particularly those related to seismic anisotropy. Grechka and Yaskevich (2013, 2014) demonstrate that it is possible to construct anisotropic velocity models from traveltimes while locating microseismic events. Their method yields more accurate source locations than those produced by conventional isotropic techniques.

Most existing algorithms invert for the seismic moment tensor $\mathbf{M}$ under the assumption that the source position $\mathbf{x}^{\mathrm{s}}$ and origin time t_0 are known. However, waveform inversion has the advantage of resolving the tensor $\mathbf{M}$ and location $\mathbf{x}^{\mathrm{s}}$ simultaneously. Here, we refine the WI algorithm for estimating the source parameters presented by Jarillo Michel and Tsvankin (2014b) and apply it to a microseismic data set recorded in a near-vertical well at Bakken field.

METHODOLOGY

Overview of the inverse problem

We consider a layered VTI model described by the interval Thomsen (1986) parameters — the P- and S-wave vertical velocities V_{P0} and V_{S0} and the anisotropy coefficients ϵ and δ. The algorithm operates with the in-plane polarized wavefield (i.e. P- and SV-waves), which is independent of the Thomsen coefficient γ. The in-plane polarized modes excited by a dislocation-type source in VTI media are governed by the components M_{11}, M_{13}, and M_{33} of the seismic moment tensor. The tensor elements depend on the fault dip θ, the fault area Σ, and the magnitude of the slip $\bar{u}$.

Our objective is to invert for the source coordinates x_1^{s} and x_3^{s}, the origin time t_0, and the three relevant moment-tensor elements assuming that the velocity model is known. Hence, the vector of model parameters is defined as:

$$\mathbf{m} = \{x_1^{\mathrm{s}}, x_3^{\mathrm{s}}, t_0, M_{11}, M_{13}, M_{33}\} \ . \tag{1}$$

The data residuals are measured by the least-squares objective function $\mathcal{F}$, which is minimized by the inversion algorithm:

$$\mathcal{F}(\mathbf{m}) = \frac{1}{2} \left\| \mathbf{d}_{\mathrm{pre}}(\mathbf{m}) - \mathbf{d}_{\mathrm{obs}} \right\|^2 , \tag{2}$$

where $\mathbf{d}_{\mathrm{pre}}(\mathbf{m})$ and $\mathbf{d}_{\mathrm{obs}}$ are the predicted and observed displacements, respectively. The displacement field $\mathbf{u}(\mathbf{x}^{\mathrm{s}}, \mathbf{x}^{\mathrm{r}_n}, t)$ in the simulations is excited by a source at $\mathbf{x}^{\mathrm{s}}$ and recorded by N receivers located at $\mathbf{x}^{\mathrm{r}_n}$ $(n = 1, 2, ..., N)$. We use finite-difference (FD) code `sfewe` in MADAGASCAR to model the 2D elastic wavefield.

We apply the adjoint-state method to efficiently calculate the gradient of the objective function with respect to the model parameters (Jarillo Michel and Tsvankin, 2014a). Although the parameters have different units, local minimization of $\mathcal{F}(\mathbf{m})$ is performed for all unknowns simultaneously using the nondimensionalization approach suggested by Kim et al. (2011) and adapted for the problem at hand by Jarillo Michel and Tsvankin (2014a). This approach eliminates the difference between the units of different parameters and makes the gradient dimensionless. Therefore, if k and $k+1$ are iteration numbers, all parameters can be updated simultaneously using a certain step length α:

$$\hat{\mathbf{m}}^{k+1} = \hat{\mathbf{m}}^{k} + \alpha\, \hat{\mathbf{g}}^{k} \ , \tag{3}$$

Line search for model updating

The inverse problem is nonlinear, and we solve it using an iterative local gradient-descent scheme. Because the true model in synthetic tests is known, it is possible to select an appropriate

DOI http://dx.doi.org/10.1190/segam2015-5929540.1

step length to achieve fast convergence. However, implementation of this approach in practice can be problematic, and it is usually more robust to compute the step length with line-search algorithms. Here, we use the following equation for the step length α described in Gauthier et al. (1986), Virieux and Operto (2009), and Pratt (2013):

$$\alpha = \frac{(\boldsymbol{\nabla}\mathcal{F})^T\mathbf{S}}{(\mathbf{JS})^T(\mathbf{JS})}\ , \tag{4}$$

where $\mathbf{S}$ is the vector of the search direction, $\mathbf{J}$ is the Fréchet matrix, and T stands for transpose. The product $\mathbf{JS}$ in the denominator of equation 4 can be approximated by perturbing the forward displacement field $\mathbf{u}(\mathbf{m})$ using a trial step length β:

$$\mathbf{JS} = \frac{\mathbf{u}(\mathbf{m}+\beta\mathbf{S}) - \mathbf{u}(\mathbf{m})}{\beta}\ . \tag{5}$$

Estimation of α is followed by minimization of the objective function and model update (equation 3) using the nonlinear conjugate gradient (NCG) method (Nocedal and Wright, 1999). Then the parameters have to be "dimensionalized" again so that they can be used as inputs for the forward modeling in the next iteration.

SYNTHETIC EXAMPLES

Test with line search

Here, we apply the line-search algorithm described above to compute the step length using the simulated wavefield. The parameters x_1^s, x_3^s, M_{11}, M_{13}, and M_{33} are estimated for the model in Figure 1; the origin time t_0 is fixed at the actual value. The objective function (Figure 2) decreases rapidly during the initial iterations. However, the convergence slows down after the ninth iteration, when the estimated source position is only about 5 m away from the actual location and the location error is smaller than the grid spacing (which in this example is 6 m). To overcome this issue, the grid size has to be defined according to the required precision in the source location. Still, the model obtained after six iterations is within the limits of seismic resolution.

Test with noise

To evaluate the influence of noise in the input data on the inversion results, we use the homogeneous VTI model from Figure 1 and add random Gaussian noise in the frequency band of the observed data with the variance equal to 0.07% of the maximum amplitude (Figure 3). Despite the significant magnitude of noise, the errors in the estimated source coordinates and the moment-tensor elements M_{11} and M_{33} are relatively small (Figure 5a,b). The inverted parameter M_{13} (Figure 5c), which is most sensitive to waveform matching, deviates by about 16% from the actual value.

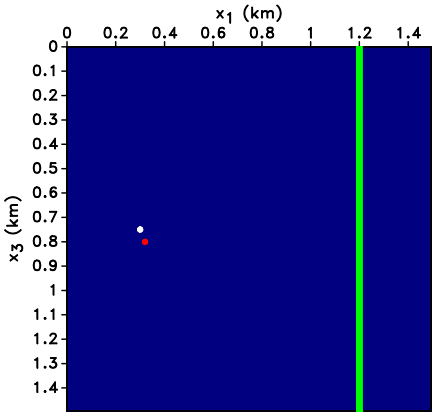

Figure 1: Actual source (white dot), trial source (red dot) and a vertical line of receivers (spacing is 6 m) embedded in a homogeneous VTI medium. The medium parameters are $\rho = 2$ g/cm^3, $V_{P0} = 4047$ m/s, $V_{S0} = 2638$ m/s, $\epsilon = 0.4$, and $\delta = 0$. The actual source is located at $x_1 = 0.3$ km and $x_3 = 0.75$ km with $\theta = 0^\circ$. For the trial source, $x_1 = 0.32$ km, $x_3 = 0.8$ km, and $\theta = 15^\circ$. Both events occur at $t_0 = 0.049$ s and have the same $\Sigma\,\bar{u} = 1$ m^3.

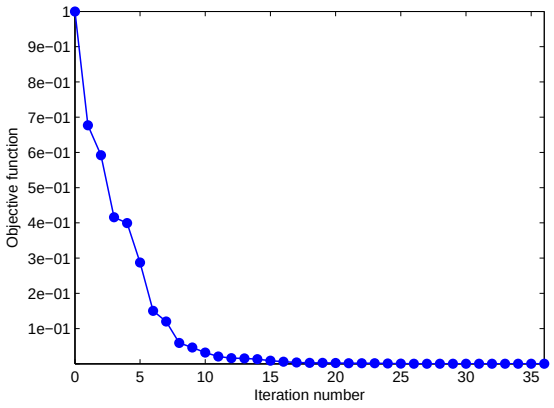

Figure 2: Change of the normalized objective function $\mathcal{F}(\mathbf{m})$ with iterations for the model in Figure 1. Parameter updating was carried out with the NCG method. The origin time t_0 is fixed at the correct value.

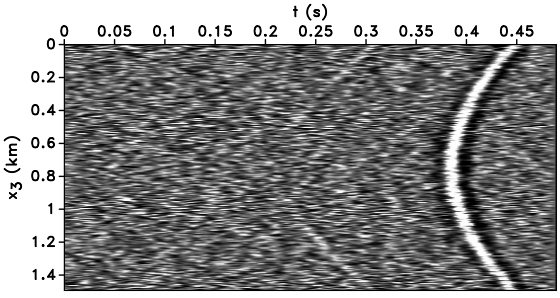

Figure 3: Vertical displacement of the observed data contaminated with Gaussian noise for the model in Figure 1. The noise has the same frequency band as the data with the variance equal to 0.07% of the maximum amplitude.

DOI http://dx.doi.org/10.1190/segam2015-5929540.1

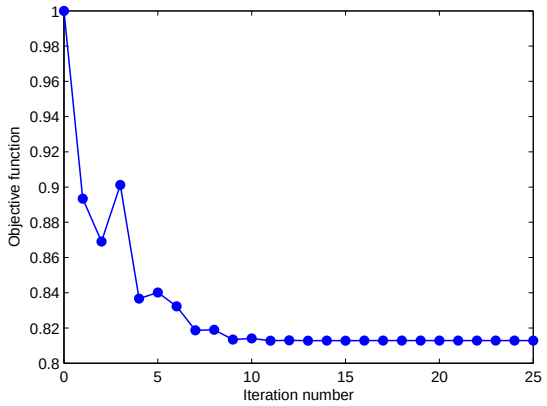

Figure 4: Change of the normalized objective function $\mathcal{F}(\mathbf{m})$ with iterations for the model in Figure 1. The inversion was performed on noise-contaminated data (see Figure 3).

MICROSEISMIC DATA SET

The microseismic survey made available to us by Marathon Oil Company was recorded at Bakken field. Conventional processing of the microseismic events was carried out by a service company that acquired the data. The events were originally located using a horizontally-layered isotropic velocity model obtained from sonic logs, perforation shots, and sleeve-opening data. The section is composed of five formations: the Lodgepole limestone (LP), Upper Bakken shales (UB), Middle Bakken sandstones and siltstones (MB), Lower Bakken shales (LB), and the Three Forks (TF) dolomites (Table 1).

Layer	V_{P0} (m/s)	V_{S0} (m/s)	ϵ	δ	γ	ρ (g/cm^3)
LP	4560	2720	0.10	0.07	0.02	2660
UB	3160	2010	0.37	-0.01	0.33	2660
MB	4630	2830	0.01	0.17	-0.12	2640
LB	2810	1970	0.27	0.19	0.35	2610
TF	4170	2380	0.09	0.16	0.13	2300

Table 1: Parameters of five layers (LP, UB, MB, LB, and TF) at Bakken field obtained by Grechka and Yaskevich (2014). The top three layers (LP, UB, MB) were found to be triclinic but the table lists the closest VTI model for each.

Here, we present inversion results for one of the strong events located by Grechka and Yaskevich (2014); data processing for other events is ongoing. Event registration was performed in two near-vertical monitor wells, one of which (with 14 receivers) is used here (Figure 6). Grechka and Yaskevich (2014) identify pronounced shear-wave splitting, with the fast S_1-wave polarized nearly horizontally (SH) and the slow S_2-wave polarized close to the vertical incidence plane (SV). We process only the P- and SV-wave (in-plane polarized) arrivals because SH-waves cannot be simulated by our modeling code. Also, we window the seismogram to focus on the direct P- and SV-waves (Figure 7). The traces for the bottom three receivers have a low signal-to-noise ratio and were removed. The ve-

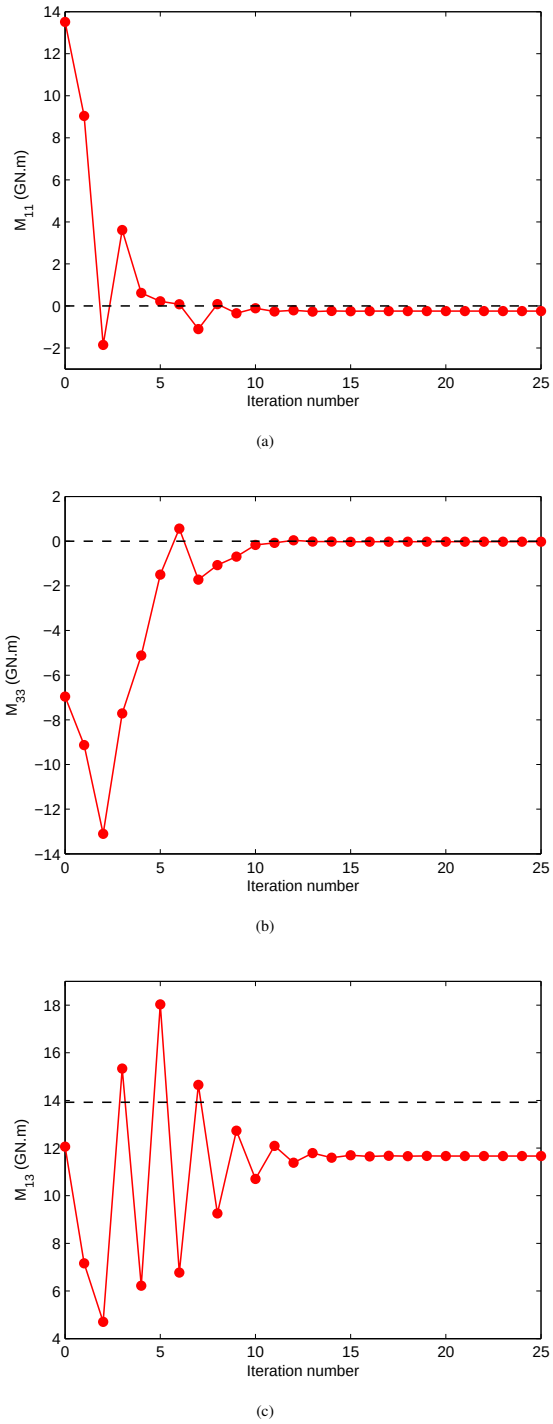

Figure 5: Change of the moment-tensor elements (a) M_{11}, (b) M_{33}, and (c) M_{13} with iterations for the model in Figure 1. The inversion was performed on noise-contaminated data (see Figure 3).

DOI http://dx.doi.org/10.1190/segam2015-5929540.1

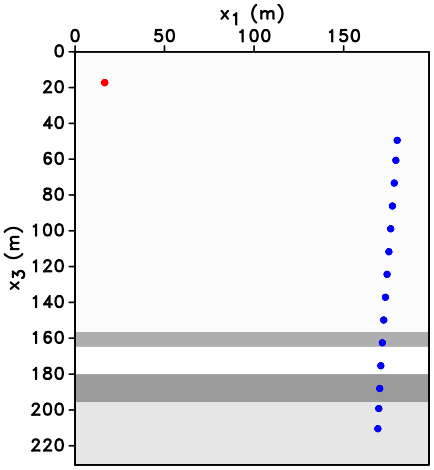

Figure 6: Acquisition geometry for the microseismic survey at Bakken field. Microseismic event (red dot) and a tilted array of receivers (blue dots) are embedded in a layered VTI medium. The average spacing between the receivers is 12.4 m. The interval medium parameters are listed in Table 1. The initial source location is $x_1 = 16.52$ m, $x_3 = 17.29$ m.

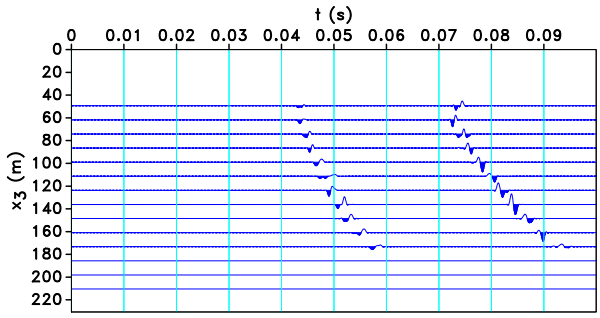

Figure 7: Vertical component of the recorded displacement after windowing of the direct P- and SV-waves.

locity model is shown in Table 1; the origin time and initial position of the source were provided to us by Dr. Grechka.

The wavelet needed for the simulation was extracted from the relatively clean P-wave arrival on the horizontal component of the fourth receiver from the top. The initial model produces significant data residuals, mostly because of a poor approximation for the moment tensor (Figure 8). After the inversion, the data fit is substantially improved and the objective function is reduced by 66%. The updated source location after the inversion is $x_1 = 14$ m, $x_3 = 16.47$ m and the estimated moment-tensor elements are $M_{11} = 4.49\text{x}10^{10}$ GN $\cdot$ m, $M_{33} = -3.22\text{x}10^{10}$ GN $\cdot$ m, and $M_{13} = 4.8\text{x}10^{10}$ GN $\cdot$ m.

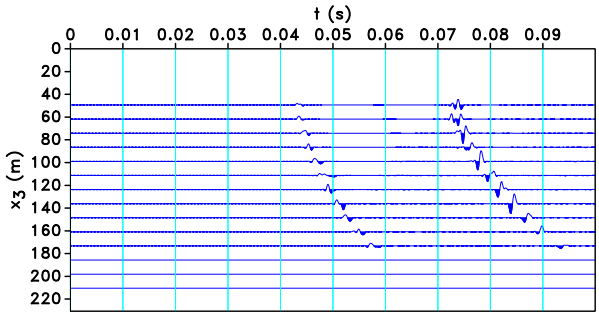

Figure 8: Difference between the recorded vertical displacement (Figure 7) and the displacement computed for the initial model. The scale is the same as in Figure 7.

CONCLUSIONS

We presented a refinement of our previously published WI method for microseismic data by introducing line search for model updates. Our algorithm is designed to estimate the parameters (location, origin time, and moment tensor) of microseismic sources for 2D elastic VTI media. Applying line search for step-length calculation improves the inversion results for field data because an optimal constant step length cannot be chosen without knowledge of the model parameters. However, line-search algorithms are subject to resolution and precision limitations related to grid spacing.

To assess the stability of the algorithm, synthetic data were contaminated with Gaussian noise in the frequency band of the signal and the variance equal to 0.07% of the maximum amplitude. The only noticeably distorted parameter (by 16%) is M_{13}. Only if the variance of the noise reaches 20% of the maximum amplitude, the inversion gets trapped in local minima.

The WI methodology is being tested on a data set from Bakken field. Although the inversion can operate with the entire seismic trace, we only use the direct P- and SV-waves due to the limitations of the velocity model. The preliminary results prove the feasibility of improving event location by matching the waveforms recorded by multicomponent receivers in a single near-vertical well.

ACKNOWLEDGMENTS

We are grateful to Vladimir Grechka (Marathon Oil), who generously provided the data set and valuable insights and feedback. The modeling and inversion results in this paper are produced with the MADAGASCAR open-source software package freely available at www.ahay.org. This work was supported by the Consortium Project on Seismic Inverse Methods for Complex Structures at the Center for Wave Phenomena (CWP).

DOI http://dx.doi.org/10.1190/segam2015-5929540.1

EDITED REFERENCES

Note: This reference list is a copyedited version of the reference list submitted by the author. Reference lists for the 2015 SEG Technical Program Expanded Abstracts have been copyedited so that references provided with the online metadata for each paper will achieve a high degree of linking to cited sources that appear on the Web.

REFERENCES

Anikiev, D., J. Valenta, F. Stanek, and L. Eisner, 2014, Joint location and source mechanism inversion of microseismic events: Benchmarking on seismicity induced by hydraulic fracturing: Geophysical Journal International, **198**, no. 1, 249–258, http://dx.doi.org/10.1093/gji/ggu126.

Gauthier, O., J. Virieux, and A. Tarantola, 1986, Two-dimensional nonlinear inversion of seismic waveforms: Numerical results: Geophysics, **51**, 1387–1403, http://dx.doi.org/10.1190/1.1442188.

Grechka, V., and S. Yaskevich, 2013, Inversion of microseismic data for triclinic velocity models: Geophysical Prospecting, **61**, no. 6, 1159–1170, http://dx.doi.org/10.1111/1365-2478.12042.

Grechka, V., and S. Yaskevich, 2014, Azimuthal anisotropy in microseismic monitoring: A Bakken case study: Geophysics, **79**, no. 1, KS1–KS12.

Jarillo Michel, O., and I. Tsvankin, 2014a, Gradient calculation for waveform inversion of microseismic data in VTI media: Journal of Seismic Exploration, **23**, no. 3, 201–217.

Jarillo Michel, O., and I. Tsvankin, 2014b, Waveform inversion for parameters of microseismic sources in VTI media: 84th Annual International Meeting, SEG, Expanded Abstracts, 1045–1049.

Kim, Y., Q. Liu, and J. Tromp, 2011, Adjoint centroid-moment tensor inversions: Geophysical Journal International, **186**, no. 1, 264–278, http://dx.doi.org/10.1111/j.1365-246X.2011.05027.x.

Nocedal, J., and S. J. Wright, 1999, Numerical optimization: Springer, http://dx.doi.org/10.1007/b98874.

Pratt, R. G., 2013, Waveform tomography: An introduction to theory and practice: Queen's University short course notes, http://geol.queensu.ca/people/pratt/Contents.pdf.

Rutledge, J. T., and W. S. Phillips, 2003, Hydraulic stimulation of natural fractures as revealed by induced microearthquakes, Carthage Cotton Valley gas field, east Texas: Geophysics, **68**, 441–452, http://dx.doi.org/10.1190/1.1567214.

Thomsen, L., 1986, Weak elastic anisotropy: Geophysics, **51**, 1954–1966, http://dx.doi.org/10.1190/1.1442051.

Virieux, J., and S. Operto, 2009, An overview of full waveform inversion in exploration geophysics: Geophysics, **74**, no. 6, WCC1–WCC26, http://dx.doi.org/10.1190/1.3238367.

Zhang, W., and J. Zhang, 2013, Microseismic migration by semblance-weighted stacking and interferometry: 83rd Annual International Meeting, SEG, Expanded Abstracts, 2045–2049.

Zhebel, O., and L. Eisner, 2015, Simultaneous microseismic event localization and source mechanism determination: Geophysics, **80**, no. 1, KS1–KS9, http://dx.doi.org/10.1190/geo2014-0055.1.

DOI http://dx.doi.org/10.1190/segam2015-5929540.1